Differential Metabolic Sensitivity of Insulin-like-response-and TORC1-Dependent Overgrowth in Drosophila Fat Cells

Maelle Devilliers, Damien Garrido, Mickael Poidevin, Thomas Rubin, Arnaud Le Rouzic, Jacques Montagne

Differential Metabolic Sensitivity of Insulin-like-response- and TORC1-Dependent Overgrowth in *Drosophila* Fat Cells

Maelle Devilliers[*], Damien Garrido[*,1,‡], Mickael Poidevin[*,‡], Thomas Rubin[*,2], Arnaud Le Rouzic[†], and Jacques Montagne[*,§]

[*] Institute for Integrative Biology of the Cell (I2BC), CNRS, Université Paris-Saclay, CEA, F-91190, Gif-sur-Yvette, France

[†] Laboratoire Evolution, Génomes, Comportement et Ecologie, CNRS, Université Paris-Saclay, UMR 9191, F-91190, Gif-sur-Yvette, France

[‡] DG and MP contributed equally to the work

[§] Author for correspondence

[1] Present address: IRIC, Université de Montréal, Montréal, Québec H3T 1J4, Canada

[2] Present address: CIRB, CNRS UMR 7241 / INSERM U-1050, F-75005 Paris Cedex 5

Running title: Metabolism and TOR signaling

Key words: Fatty acid synthesis, Glycolysis, cell-autonomous effect, homeostasis

Corresponding author:

Jacques Montagne

Institute for Integrative Biology of the Cell (I2BC), CNRS, Université Paris-Saclay, CEA,

Bâtiment 21, Avenue de la Terrasse

F-91190, Gif-sur-Yvette, France

+33 (0) 1 6982 4607

Jacques.MONTAGNE@i2bc.paris-saclay.fr

ABSTRACT

Glycolysis and fatty acid (FA) synthesis directs the production of energy-carrying molecules and building blocks necessary to support cell growth, although the absolute requirement of these metabolic pathways must be deeply investigated. Here, we used *Drosophila* genetics and focus on the TOR (Target Of Rapamycin) signaling network that controls cell growth and homeostasis. In mammals, mTOR (mechanistic-TOR) is present in two distinct complexes, mTORC1 and mTORC2; the former directly responds to amino acids and energy levels, whereas the latter sustains insulin-like-peptide (Ilp) response. The TORC1 and Ilp signaling branches can be independently modulated in most *Drosophila* tissues. We show that TORC1 and Ilp-dependent overgrowth can operate independently in fat cells and that ubiquitous over-activation of TORC1 or Ilp signaling affects basal metabolism, supporting the use of *Drosophila* as a powerful model to study the link between growth and metabolism. We show that cell-autonomous restriction of glycolysis or FA synthesis in fat cells retrains overgrowth dependent on Ilp- but not TORC1-signaling. Additionally, the mutation of *FASN* (Fatty acid synthase) results in a drop in TORC1 but not Ilp signaling, whereas, at the cell-autonomous level, this mutation affects none of these signals in fat cells. These findings thus, reveal differential metabolic sensitivity of TORC1- and Ilp-dependent growth and suggest that cell-autonomous metabolic defects might elicit local compensatory pathways. Conversely, enzyme knockdown in the whole organism results in animal death. Importantly, our study weakens the use of single inhibitors to fight mTOR-related diseases and strengthens the use of drug combination and selective tissue-targeting.

INTRODUCTION

The mTOR (mechanistic Target Of Rapamycin) regulatory network orchestrates organismal growth in response to growth factor signaling and nutritional status (LAPLANTE AND SABATINI 2012; HOWELL *et al.* 2013; LAMMING AND SABATINI 2013; SHIMOBAYASHI AND HALL 2014; CARON *et al.* 2015; SAXTON AND SABATINI 2017; MOSSMANN *et al.* 2018). Activation of this network promotes basal cellular functions, thereby providing building blocks to sustain cellular growth. However, despite a plethora of studies on the mTOR signaling network, the requirement of basal metabolism— glycolysis and FA synthesis— for cell growth has not been systematically investigated. The *Drosophila* model provides a powerful genetic system to address these issues (UGUR *et al.* 2016), since both the intermediates of this signaling network and the basal metabolic pathways are conserved in the fruit fly (MONTAGNE *et al.* 2001; HAY AND SONENBERG 2004; PADMANABHA AND BAKER 2014; ANTIKAINEN *et al.* 2017; WANGLER *et al.* 2017; LEHMANN 2018).

The mTOR protein kinase is present in two distinct complexes, mTORC1 and mTORC2 that comprise raptor and rictor, respectively (KIM *et al.* 2002; SARBASSOV *et al.* 2005). ATP and amino acid levels control the recruitment of an mTORC1 homodimer at the lysosomal membrane in the vicinity of the small GTPase Rheb (Ras homologue enriched in brain) (GOBERDHAN *et al.* 2009; MA AND BLENIS 2009; DIBBLE AND MANNING 2013; GROENEWOUD AND ZWARTKRUIS 2013; MONTAGNE 2016). Rheb stimulates mTORC1 activity (YANG *et al.* 2017), which in turn regulates several downstream targets. S6Kinase1 (S6K1) is one such kinase, sequentially activated through the phosphorylation of its T389 and T229 residues by mTORC1 and by PDK1 (Phosphoinositide-dependent protein kinase 1), respectively (MONTAGNE AND THOMAS 2004; MAGNUSON *et al.* 2012). Rheb activation of mTORC1 is repressed by the tumor

suppressor TSC (Tuberous sclerosis complex) that comprises subunits TSC1 and TSC2 (RADIMERSKI *et al.* 2002a; GARAMI *et al.* 2003; INOKI *et al.* 2003a; DIBBLE *et al.* 2012). The integrity of mTORC2 is required to sustain the downstream insulin-signaling response (SARBASSOV *et al.* 2005). Binding of insulin or related peptides (Ilps) to their cognate receptors results in recruitment of class I PI3K (Phosphoinositide 3-kinase) to the membrane. PI3K phosphorylates inositol lipids to phosphatidylinositol-3,4,5-triphosphate (PIP3) (ENGELMAN *et al.* 2006; HAEUSLER *et al.* 2018), while the tumor suppressor PTEN counteracts this process (CULLY *et al.* 2006; GOBERDHAN *et al.* 2009). PIP3 constitutes a membrane docking site for the protein kinase Akt whose activity requires the subsequent phosphorylation of its S473 and T308 residues by mTORC2 and PDK1, respectively (LIEN *et al.* 2017).

Constitutive activation of mTORC1 in MEFs (Mouse embryonic fibroblasts) represses the tricarboxylic acid (TCA) cycle and stimulates anaerobic glycolysis and biosynthesis of FAs and cholesterol (DUVEL *et al.* 2010). Conversely, adipose-specific knockout of raptor to impede mTORC1 formation, results in enhanced uncoupling of mitochondrial activity (POLAK *et al.* 2008). The increased lipogenesis observed in mTORC1 stimulated cells depends on the cofactor Lipin 1 and on a SREBP (Sterol responsive element binding-protein) family member (DUVEL *et al.* 2010; PETERSON *et al.* 2011). Congruently, TSC2 mutant cells become addicted to glucose as a result of mTORC1 hyper-activity (INOKI *et al.* 2003b) and, in the context of mTORC1 inhibition, promote glutamine anaplerosis (CHOO *et al.* 2010; CSIBI *et al.* 2013; CSIBI *et al.* 2014). Ilp-signaling also impinges on basal metabolism. Intracellular activation of Akt increases ATP levels (HAHN-WINDGASSEN *et al.* 2005; ROBEY AND HAY 2009) through the stimulation of GLUT4-mediated glucose uptake (JALDIN-FINCATI *et al.* 2017) and the enhancement of the expression and activity of glycolytic enzymes (GOTTLOB *et al.* 2001; HOUDDANE *et al.*

2017). Akt also dampens glucose production by suppressing PEPCK (gluconeogenesis), glucose-6-phosphatase (glycogenolysis) and the glycogen synthesis repressor GSK3 (NAKAE *et al.* 2001; MCMANUS *et al.* 2005). In addition, Akt promotes mitochondrial metabolism and oxidative phosphorylations (GOTTLOB *et al.* 2001; MAJEWSKI *et al.* 2004). Conversely, hepatic knockout of the mTORC2 specific-subunit rictor results in constitutive gluconeogenesis and impaired glycolysis and lipogenesis (HAGIWARA *et al.* 2012; YUAN *et al.* 2012). Taken together, these studies strongly emphasize the role of mTOR in metabolic-related diseases and in adjusting metabolism to the nutritional and energy status (MOSSMANN *et al.* 2018).

Despite a plethora of studies, the net requirement of these metabolic changes to sustain overgrowth induced by over-activation of mTOR signaling has not been formally addressed. This signaling network is conserved in *Drosophila* (hereafter called as TOR), providing a powerful genetic system to address these issues. In the present study, we investigated the requirement of glycolysis and FA synthesis for the cellular growth induced by hyper-activation of TORC1 signaling and Ilp response in *Drosophila*. Consistent with previous studies (RADIMERSKI *et al.* 2002a; RADIMERSKI *et al.* 2002b; DONG AND PAN 2004; MONTAGNE *et al.* 2010; PALLARES-CARTES *et al.* 2012), we show that TORC1- and Ilp-dependent overgrowth can be independently modulated in the *Drosophila* fat body (FB), the organ that fulfils hepatic and adipose functions (PADMANABHA AND BAKER 2014; ANTIKAINEN *et al.* 2017; LEHMANN 2018). We show that ubiquitous over-activation of TORC1 or Ilp signaling affects basal metabolism and that metabolic restriction at the organismal level has dramatic consequences on animal survival, but minor effect at the cell-autonomous level. This suggests that within an organism, alternative strategies may operate to compensate local metabolic defects. Finally, at the cell-autonomous level, metabolic restriction can partially restrain

overgrowth dependent on hyper-activation of Ilp- but not TORC1-signaling, indicating that the potential compensatory metabolic pathways do not fully operate in the context of Ilp-signaling stimulation.

MATERIAL & METHODS

Genetics and fly handling

Fly strains: *P[w[+mC]=tubP-GAL80]LL10,P[ry[+t7.2]=neoFRT]40A*, *daughterless(da)-gal4*, *tub-gal80^{ts}*, *UAS-Dcr-2* (Bloomington Stock Center); *hs-flp,tub-gal4,UAS-nls-GFP/FM7*, *FASN$^{1-2}$* (GARRIDO *et al.* 2015); *Tor$^{\Delta P}$* (ZHANG *et al.* 2000); *Tor^{2L1}*, *Tor^{2L19}* and *PTEN* (OLDHAM *et al.* 2000); *EP(UAS)-Rheb* (STOCKER *et al.* 2003); inducible interfering RNA (*UAS-RNAi*) lines to *PTEN* (NIG 5671R-2), *FASN1* (VDRC 29349), *PFK1* (VDRC 3017), *PK* (VDRC 49533) *PDH* (VDRC 40410), *LDH* (VDRC 31192) (DIETZL *et al.* 2007). To generate MARCM clones in a *Minute* background, the *FRT40/P(arm-LacZ w^{+})* chromosome (BOHNI *et al.* 1999) was recombined with the *P[w[+mC]=tubP-GAL80]LL10,P[ry[+t7.2]=neoFRT]40A* chromosome (LEE AND LUO 2001). Standard media: agar (1g), polenta (6g) and yeast (4g) for 100ml. Lipid- (beySD) and sugar-complemented media were as described (GARRIDO *et al.* 2015). *FASN$^{1-2}$* mutant larvae were collected at L1 hatching on grape juice plates following the lack a GFP-labelled balancer and transferred to fresh tubes. Prepupae were collected once a day to evaluate developmental delay and to measure body weight and size.

Molecular biology and Biochemistry

RNAi-knockdown efficacy (Figure S1): *UAS-Dcr-2;da-gal4,tub-gal80^{ts}* females mated with UAS-RNAi males were let to lay eggs overnight. tubes were kept at 19°C for two

days, then transferred at 29°C; two days later, larvae of roughly the same size were collected for quantitative PCR as described (PARVY *et al.* 2012). For western-blotting, protein extracts were prepared as described and antibodies were previously described for dS6K and phospho-S6 (MONTAGNE *et al.* 2010; ROMERO-POZUELO *et al.* 2017) or commercially provided for phospho-dS6K, Akt and ERK (Cell signaling 9209, 9272, 4054, 4695, 4370).

For metabolic measurements, tubes containing 24-hr egg collection were maintained at 29°C to strengthen the gal4/UAS effect. Larvae were selected prior to L2/L3 transition and transferred on either a standard diet or a 20%-SSD. Collection of prepupae and metabolic measurements were performed as described (GARRIDO *et al.* 2015). For protein and TAG measurements, prepupae were weighted and crushed in 400 µl PBT (PBS, 0.1% Triton X-100) and centrifuged for 5 mn at 12000 rpm. For proteins, 10 µl of extract mixed with 1 ml of 5X-diluted reagent (Bio-Rad Protein Assay Kit) were incubated 15 mn in dark at room temperature; OD was measured at 595 ηm. For TAGs, 20 µl of extract mixed with 500 µl of reagent (Kit STANBIO Triglyceride LiquiColor) were incubated 15 mn at 37°C; OD was measured at 500 ηm. For trehalose and glycogen, prepupae were crushed in 350 µl $Na_2CO_3^-$ (0,25 M) (PBS 0.1% Triton X-100). After 2 hrs incubation at 65°C, 700 µl of Na Acetate (0.3 M) and 130 µl of Acetic acid (1.7 M) were added and tubes were centrifuged for 10 mn at 12000 rpm. For each sample, three sets of 20 µl of extract were incubated overnight at 37°C, two of them contained 1 U/ml of either Trehalase or Amyloglucosidase (SIGMA). Next, all samples mixed with 500 µl of glucose oxidase (Thermo Electron, GLUCOSE (GDO-POD)) were incubated 20 mn at 37°C; OD was measured at 510 ηm. The net concentration of trehalose and glycogen was obtained by subtracting the concentration values of the extracts without enzyme.

Clonal analysis

MARCM clones (LEE AND LUO 2001) were generated from 6-7hr egg collections heat-shocked for 65 mn at 38°C. FB of late L3 feeding larvae where dissected, fixed and labelled with Phalloidin (membranes) and DAPI (nuclei) as described (GARRIDO *et al.* 2015). Image were acquired on a Leica SP8 confocal laser-scanning microscope. Cell size calculation has been performed as described (GARRIDO *et al.* 2015) from at least eight larvae per genotype, containing a few MARCM clones surrounded by control cells. Because of an extremely low ratio of larvae that fully develop and harbour mitotic clones, the mean values were calculated from several experiments that could not be performed at the same time, but over a long period. Therefore, for the graphs of cell size measurement (Figures S2A, S2C, 5M and 7M), values are reused when they correspond to the same genotype and conditions, allowing direct comparison between experiments.

Data and reagent availability statement

Fly stocks and reagents are available upon request. Supplementary materials include Figures S1-S5, statistical analysis (methods and Tables S1-S7) and supdata/script files.

RESULTS

TORC1 and Ilp signaling independency in the fat body

To investigate the relationship between TORC1- and Ilp-dependent overgrowth in the FB, we generated somatic clones either over-expressing Rheb (*Rheb*$^{+}$) (STOCKER *et al.*

2003) or *PTEN* homozygous mutants (*PTEN*$^{-/-}$) (OLDHAM *et al.* 2000). The precursors of FB cells divide in the embryo; during larval life, the differentiated cells do not divide but endoreplicate their DNA content to reach a giant size (EDGAR AND ORR-WEAVER 2001). Therefore, to precisely evaluate the effect on cell growth, somatic recombinations were induced during embryogenesis at the stage of proliferation of the FB cell precursors and the resulting MARCM clones were analyzed in the FB of late feeding L3 larvae, prior to the wandering stage that precedes metamorphosis entry. In accordance with previous studies manipulating Ilp and TOR signaling in FB cells (BRITTON *et al.* 2002; SCOTT *et al.* 2004), both *PTEN*$^{-/-}$ and *Rheb*$^{+}$ clonal cells were bigger than the surrounding control cells and this cell size effect was dramatically increased in *PTEN*$^{-/-}$;*Rheb*$^{+}$ combined clones (Figure 1A-D and Figure S2A). We next analyzed this growth increase in the context of previously reported *Tor* mutations, the *Tor*$^{\Delta P}$ deletion (ZHANG *et al.* 2006), and the *Tor*^{2L1} and *Tor*^{2L19} alleles that result in a kinase inactive and in a short truncated protein, respectively (OLDHAM *et al.* 2000). Given that we could not find mutant clones, which were likely eliminated by cell competition, we generated somatic clones in a *Minute* background to slow down the growth of the surrounding control cells. In these conditions, any of the *Tor* mutant cells exhibited a dramatic size reduction (Figure 1G, 1J, 1M and Figure S2C) and this phenotype was dominant in *Rheb*$^{+}$ combined clonal cells (Figure S2C and compare Figure 1E to 1H, 1K and 1N). In contrast, *Tor*$^{\Delta P}$ and *Tor*^{2L19} but not *Tor*^{2L1} exhibited a clear dominant phenotype over the *PTEN*$^{-/-}$ mutation; the size of *Tor*$^{\Delta P}$,*PTEN*$^{-/-}$ and *Tor*^{2L19},*PTEN*$^{-/-}$ clonal cells was dramatically reduced (Figure S2C and compare Figure 1F to 1L and 1O), whereas *Tor*^{2L1},*PTEN*$^{-/-}$ clonal cells were bigger than the surrounding cells (Figure 1M) and tend to be relatively bigger than control clonal cells (Figure S2B and S2C). These findings indicate that the *Tor*^{2L1}

mutation restrains TORC1- but not Ilp-dependent overgrowth, whereas $Tor^{\Delta P}$ and Tor^{2L19} affects both.

Next, we used phospho-specific antibodies in immunostaining assays to analyze the phosphorylation of Akt (P-Akt) and of the dS6K target, ribosomal protein rpS6 (P-S6). The P-Akt intracellular signal was increased in $PTEN^{-/-}$ clones, absent in $Tor^{\Delta P}$ and Tor^{2L19} clones, but not affected in Tor^{2L1} clones (Figure 2A-D). Staining with the rpS6 phospho-specific antibody revealed a patchy signal, with only a subset of cells expressing the P-S6 signal in the FB (Figure 2E-H), a pattern previously described in the wing imaginal disc (ROMERO-POZUELO *et al.* 2017). Therefore, to evaluate TORC1 activity, we measured the ratio of P-S6 positive cells among the population of GFP^+ clonal cells. About half of the control clones were P-S6 positive (Figure 2E and 2M), whereas most of the Tor^{2L1}, Tor^{2L19} and $Tor^{\Delta P}$ clones were P-S6 negative (Figure 2F-H and 2M). Importantly, almost all the $Rheb^+$ clones were P-S6 positive (Figure 2I and 2M), whereas the ratio of P-S6 positive cells was slightly but not significantly increased in the $PTEN^{-/-}$ clones (Figure 2J and 2M). Taken together, these findings reveal that the Tor^{2L1} mutation affects only TORC1, whereas the $Tor^{\Delta P}$ and Tor^{2L19} mutations affect both signaling branches and support the notion that Ilp- and TORC1-dependent overgrowth can be independently modulated in FB cells.

Activating TORC1 or Ilp signaling impacts basal metabolism

To evaluate how TORC1 and Ilp affect basal metabolism in *Drosophila*, we analyzed various metabolites in whole animals that express the ubiquitous *da-gal4* driver to direct Rheb overexpression ($Rheb^{++}$) or PTEN knockdown (*PTEN-RNAi*). Larvae were fed either a standard or a 20%-sucrose supplemented diet (20%-SSD) and 0-5h prepupae were collected, as this is a convenient phase to stage the animals after the feeding

period. When fed a standard diet, a high rate of lethality was observed for *Rheb*$^{++}$ and *PTEN-RNAi* larvae, although a sufficient number of prepupae could be recovered. Given that none of the *Rheb*$^{++}$ and *PTEN-RNAi* larvae fed a 20%-SSD reached the prepupal stage, larvae were first fed a standard diet and transferred onto a 20%-SSD at the L2/L3 molting transition. In this way, we could recover a few prepupae for metabolic measurements. For both males and females fed a standard diet, the body weight of *Rheb*$^{++}$ and *PTEN-RNAi* prepupae was roughly similar to that of controls (Figure 3A and 3B). Conversely, providing a 20%-SSD resulted in a drop of the prepupal weight of control animals that was significantly compensated in *Rheb*$^{++}$ and *PTEN-RNAi* prepupae (Figure 3A and 3B).

Next, we measured the total amounts of protein, triacylglycerol (TAG), glycogen and trehalose—the most abundant circulating sugar in *Drosophila*. Although protein levels did not vary in *PTEN-RNAi* and *Rheb*$^{++}$ animals fed a standard diet, a mild but significant increase was observed in *PTEN-RNAi* animals fed a 20%-SSD (Figure 3C). TAG levels were strongly increased in animals fed a 20%-SSD (Figure 3D). When fed a standard diet, TAG levels did not vary in *PTEN-RNAi* and *Rheb*$^{++}$ animals, whereas, when fed a 20%-SSD, they were strongly increased in *PTEN-RNAi* animals (Figure 3D). Feeding larvae a 20%-SSD resulted in a moderate increase in glycogen and trehalose levels in control prepupae (Figure 3E-F). In *Rheb*$^{++}$ and, in lower extent, in *PTEN-RNAi* prepupae, glycogen levels were significantly lower than those measured in controls (Figure 3E). Finally, trehalose levels were strongly decreased in both *Rheb*$^{++}$ and *PTEN-RNAi* prepupae fed either a standard or a 20%-SSD as compared to control (Figure 3F). Taken together, these findings suggest that a ubiquitous increased activity of either TORC1 or Ilp signaling provokes an apparent increase in sugar consumption. This metabolic rate is correlated with a relative increase in body weight for larvae fed a

20%-SSD, but not for those fed a standard diet. We previously observed that increasing dietary sucrose induced a reduction in food intake (GARRIDO *et al.* 2015) that may account for the body weight reduction of control animals. Potentially, food intake could be less affected in *Rheb*$^{++}$ and *PTEN-RNAi* animals, thereby leading to a compensatory effect on body weight. Measuring food intake in *Rheb*$^{++}$ or *PTEN-RNAi* larvae was not applicable since most of them die during larval stage and thus, terminate feeding earlier. In sum, our data indicates that basal metabolism is altered in the few *Rheb*$^{++}$ or *PTEN-RNAi* larvae that survive and further suggests that in most cases stronger metabolic disruption may happen, resulting in lethal homeostatic defects.

Knocking-down glycolysis at the whole body level

To determine whether the basal energy metabolism affected TORC1- and/or Ilp-signaling, we ubiquitously expressed RNAis against phosphofructokinase1 (*PFK1-RNAi*), pyruvate kinase (*PK-RNAi*) pyruvate dehydrogenase (*PDH-RNAi*) and lactate dehydrogenase (*LDH-RNAi*). PFK1 catalyzes the third glycolytic reaction to form fructose 1,6-bisphophate; PK catalyzes the final glycolytic reaction to form pyruvate; PDH directs the mitochondrial fate of pyruvate, whereas LDH directs its anaerobic fate (Figure 4A). When directed with the ubiquitous *da-gal4* driver, *PK-RNAi* provoked early larval lethality, *PFK1-RNAi* and *PDH-RNAi* provoked larval lethality at L2 or L3 stages, whereas *LDH-RNAi* induced a semi-lethal phenotype at larval or pupal stages (Figure 4B).

Next, we monitored the phosphorylation of the *Drosophila* S6Kinase (dS6K), Akt and ERK. To circumvent the early lethality, the activity of the *da-gal4* driver was blocked until early L1 stage using the thermo-sensitive Gal4 inhibitor, Gal80^{ts}, then, RNAi expression was induced by a temperature shift at 29°C; protein extracts were prepared

two days later using late L2 larvae. At this stage the larvae were still viable, although those expressing PK-RNAi did not undergo L2/L3 transition and eventually died (Figure 4B). Western-blotting revealed that RNAi-knockdown of PFK1 or LDH did not affect phosphorylation of dS6K, Akt or ERK (Figure 4C and Figure S3A-F). In contrast, knockdown of PK or PDH decreased dS6K phosphorylation, whereas PK- but not PDH-knockdown mildly decreased Akt phosphorylation (Figure 4C and S3A-D). Unexpectedly, knockdown of PK and LDH, and in lower extent knockdown of PFK and PDH, increased the amounts of total ERK protein with minor effects on its phosphorylation rate (Figure 4C and Figure S3E-F). These results indicate that ubiquitous knockdown of aerobic glycolysis specifically affects TORC1 signaling.

To evaluate the requirement of glycolysis for adult survival, RNAi-knockdown was induced by temperature shift to 29°C in newly emerged flies and lethality was counted every second day. In both males and females, PK and PFK1 knockdown provoked lethality between 10 to 14 days after temperature shift (Figure 4D). Knockdown of PDH and LDH also induced adult lethality, although not as soon as PK and PFK1 knockdown (Figure 4D). As a comparison, to evaluate the consequence of disrupting FA synthesis, we knocked-down FASN1 (Figure 4A) in adults; about a quarter of *FASN1-RNAi* flies died between 10 to 14 days, while the others survived nearly as well as control flies (FASN1i in Figure 4D). Taken together, these data indicate that glycolysis is essential for both larval development and adult survival.

Cell-autonomous requirement of glycolysis for Ilp- but not TORC1-dependent overgrowth

To investigate the requirement of glycolysis to sustain cell-autonomous overgrowth dependent on Ilp- and TORC1-signaling, *PFK1-RNAi*, *PK-RNAi*, *PDH-RNAi* and *LDH-*

RNAi were induced in *PTEN*$^{-/-}$ or *Rheb*$^{+}$ clones. Except a moderate effect of *PK-RNAi*, clones expressing RNAi against these metabolic enzymes did not significantly affect the growth of FB cells (Figure 5A-D and 5M). In combined clones, none of the RNAi affected the growth of *Rheb*$^{+}$ clones (Figure 5E-H and 5M). In contrast, the size of *PTEN*$^{-/-}$ clones was significantly decreased when co-expressing RNAi against any of these metabolic enzymes (Figure 5I-M). These findings indicate that both aerobic and anaerobic glycolysis are required to sustain cell-autonomous overgrowth dependent on Ilp signaling. In contrast, reducing glycolysis does not counteract cell-autonomous overgrowth dependent on TORC1 signaling.

Linking FA synthesis to TORC1- and Ilp-signaling

Since glycolysis and FA synthesis are tightly connected metabolic pathways (GARRIDO *et al.* 2015), we investigated whether the deficiency of the latter affects Ilp or TORC1 signaling. The *Drosophila* genome encodes three *FASN* genes, *FASN1* is ubiquitously expressed but not *FASN2* or *FASN3* (PARVY *et al.* 2012; CHUNG *et al.* 2014; WICKER-THOMAS *et al.* 2015). The deletion of the *FASN1* and *FASN2* tandem (*FASN*$^{\Delta 24\text{-}23}$ deletion, hereafter called *FASN*$^{1\text{-}2}$) results in a lethal phenotype that can be rescued by feeding larvae a lipid-complemented diet (beySD) (GARRIDO *et al.* 2015; WICKER-THOMAS *et al.* 2015). However, beySD-rescued *FASN*$^{1\text{-}2}$ mutant larvae exhibited a developmental delay to enter metamorphosis (Figure 6A). Further, when beySD-rescued *FASN*$^{1\text{-}2}$ mutant larvae were transferred at the L2/L3 larval transition onto a 10% sucrose-supplemented-beySD, only a few of them completed the third larval stage and, after an extreme developmental delay, entered metamorphosis (Figure 6A). Delay in development can be due to a default in ecdysone production that results in giant pupae (PARVY *et al.* 2014) or to impaired TOR signaling that results in reduced body

growth (MONTAGNE *et al.* 1999; OLDHAM *et al.* 2000). Measurements of prepupal weight revealed that *FASN*$^{1-2}$ mutant prepupae exhibited a severe reduction in body weight and body size, whether or not they were supplemented with sucrose (Figure 6B and Figure S4), suggesting a defect in TOR signaling. Therefore, we analyzed the phosphorylation of the *Drosophila* S6Kinase (dS6K) and Akt in protein extracts of late feeding L3 larvae. Western-blotting revealed that the dS6K protein resolved in several bands in *FASN*$^{1-2}$ extracts, whereas Akt protein was unchanged (Figure 6C and Figure S3G and S3I). These results suggest that dS6K but not Akt might be degraded in the *FASN*$^{1-2}$ mutant background. In addition, dS6K phosphorylation decreased in *FASN*$^{1-2}$ extracts and became barely detectable when *FASN*$^{1-2}$ larvae were fed a sucrose-supplemented-beySD (Figure 6C and Figure S3H). Conversely, the phosphorylation of Akt was unaffected in larvae fed a beySD, although it was slightly decreased in larvae fed a sucrose-supplemented-beySD (Figure 6C and Figure S3J). This finding contrasts with our previous observation showing that FB explants of *FASN*$^{1-2}$ mutant larvae were hypersensitive to insulin (GARRIDO *et al.* 2015). However, *FASN*$^{1-2}$ mutants also exhibited a decrease in food intake (GARRIDO *et al.* 2015), which might induce a systemic suppression of dS6K phosphorylation, while FB explant were cultured in nutrient media supplemented with insulin. Therefore, to determine whether *FASN* mutation affects TOR signaling at the cell-autonomous level, we analyzed P-S6 and P-Akt in *FASN*$^{1-2}$ mutant clones in the FB. As for control clones, about half of the *FASN*$^{1-2}$ clonal cells were P-S6 positive (Figure 2L and 2M). Furthermore, no effect on P-Akt was observed in *FASN*$^{1-2}$ clonal cells (Figure 2K). In summary, these findings reveal that disrupting FA synthesis does not significantly affect TORC1 and Ilp signaling at the cell-autonomous level, although it seems to impinge on TORC1 signaling when inhibited in the whole animal whether directly or indirectly.

Cell-autonomous requirement of FA synthesis for Ilp- but not TORC1-dependent overgrowth

To determine, whether FA synthesis is required at the cell-autonomous level to sustain TORC1 and/or Ilp dependent growth, we analyzed *FASN*$^{1-2}$ clones while enhancing either TORC1 or Ilp signaling in FB cells. We previously reported (GARRIDO *et al.* 2015) that *FASN*$^{1-2}$ clonal cells in the FB were slightly reduced in size and that this effect was dramatically increased in larvae fed a 20%-SSD (Figure S5A-B and Figure 7M). Therefore, we generated *PTEN*$^{-/-}$ and *Rheb*$^{+}$ clones combined or not with the *FASN*$^{1-2}$ mutation and analyzed them in the FB of larvae fed either a standard diet or a 20%-SSD. As compared to the standard diet, feeding larvae a 20%-SSD had no effect on the size of *Rheb*$^{+}$ clonal cells, but significantly reduced the size of *PTEN*$^{-/-}$ and of *PTEN*$^{-/-}$;*Rheb*$^{+}$ clonal cells (Figure 7A-F and 7M). Further, when combined with the *FASN*$^{1-2}$ mutation, *PTEN*$^{-/-}$ but not *Rheb*$^{+}$ clones were significantly reduced in size (Figure 7G-H and 7M). The *FASN*$^{1-2}$ mutation also provoked a severe size reduction of *PTEN*$^{-/-}$,*Rheb*$^{+}$ clones (Figure 7I and 7M). Moreover, as compared to the standard diet, feeding larvae a 20%-SSD induced a significant size reduction of *FASN*$^{1-2}$;*Rheb*$^{+}$, *FASN*$^{1-2}$,*PTEN*$^{-/-}$ and *FASN*$^{1-2}$,*PTEN*$^{-/-}$;*Rheb*$^{+}$ clonal cells (Figure 7J-L and 7M). Of note, except for the *FASN*$^{1-2}$;*Rheb*$^{+}$ clonal cells in larvae fed a 20%-SSD that exhibited a size roughly identical to that of the surrounding control cells (Figure 7J), the cell size was always bigger than the controls (Figure 7M). These findings indicate that, in larvae fed a standard diet, FA synthesis is at least in part required to sustain over-growth induced by Ilp, but not TORC1. Nonetheless, the metabolic dependency of Ilp-induced overgrowth might be a consequence of the stronger phenotype of *PTEN*$^{-/-}$ clones, which could be more sensitive to metabolic restriction than the one of *Rheb*$^{+}$ clones. To challenge such

an unspecific effect, we made use of *PTEN-RNAi* that diminish but do not abolish its expression. In this setting, the size of *PTEN-RNAi* clonal cells was significantly higher than the one of control clones, but not as much as the one of *Rheb*$^{+}$ clonal cells (Figure 7M and Figure S5C). Importantly the size of *PTEN-RNAi* clonal cells was significantly diminished when combine to the *FASN* deficiency (Figure 7M and Figure S5D), which excludes a strength-phenotype dependent effect. In conclusion, overgrown cells generated by Ilp over-activation have limited homeostatic abilities to adjust to metabolic restriction, whereas TORC1 activated cells at least in part maintain these abilities.

DISCUSSION

In this study, we have investigated the functional links between the glycolysis/FA synthesis axis and TORC1- or Ilp-dependent growth in *Drosophila*. Consistent with previous studies (RADIMERSKI *et al.* 2002a; RADIMERSKI *et al.* 2002b; DONG AND PAN 2004; MONTAGNE *et al.* 2010; PALLARES-CARTES *et al.* 2012), we show that TORC1- and Ilp-dependent overgrowth can be independently modulated in the *Drosophila* FB. TORC1, once recruited at the lysosomal membrane, is activated by Rheb to phosphorylate downstream targets (MONTAGNE 2016). TORC2, which comprises rictor, resides in the Ilp signaling cascade to phosphorylate the S505 residue in the hydrophobic motif (HM) of Akt. However, a study on a *Drosophila rictor* mutant reported that S505 phosphorylation by TORC2 was not required to sustain Akt-dependent growth and proposed that TORC2 plays as a rheostat for this process (HIETAKANGAS AND COHEN 2007). Here, we provide evidence that the previously described *Tor*^{2L1} mutation, which likely results in a kinase-inactive protein (OLDHAM *et al.* 2000), affects TORC1 but not Ilp-dependent overgrowth, whereas both overgrowth processes are suppressed by the *Tor*$^{\Delta P}$ or *Tor*^{2L19} mutations that likely represent null mutants. Surprisingly, we observe

427 that the S505 residue in the Akt HM is still phosphorylated in *Tor*^{2L1}, but not *Tor*$^{\Delta P}$ and
428 *Tor*^{2L19} mutant clones. Taken together, these findings reveal that the TOR protein, but
429 not its kinase activity, is required for Akt HM phosphorylation and for Ilp-dependent
430 overgrowth through a molecular mechanism that remains to be elucidated.

431 Intriguingly, our study reveals apparent contradictory effects between perturbations at
432 the whole body and cell-autonomous levels. At the organismal level, knockdowns of
433 glycolytic enzymes to mimic drug treatment with a systemic inhibitor result in animal
434 death. Knockdown of PDH suppress dS6K but not Akt phosphorylation suggesting that
435 aerobic glycolysis is crucial for TORC1 signaling. These observations contrast with
436 mammalian studies showing that mTORC1 stimulation promotes anaerobic glycolysis
437 (DUVEL *et al.* 2010), whereas Akt activation promotes aerobic glycolysis (GOTTLOB *et al.*
438 2001). Furthermore, at the cell-autonomous level, repression of either aerobic or
439 anaerobic glycolysis partly restrains Ilp- but not TORC1-dependent overgrowth of FB
440 cells. Taken together, these findings confirm the existence of tight connections between
441 TOR signaling and basal metabolism, although the cell-autonomous effects suggest that
442 this connection integrates interactions operating between neighboring cells or organs. In
443 addition, the growth defect of beySD-rescued *FASN* null mutants might result from the
444 decrease in TORC1 activity, suggesting that TORC1 but not Ilp signaling relies on FA
445 synthesis. However, at the cell autonomous level, the deficiency of *FASN* restrains Ilp
446 but not TORC1 dependent overgrowth in FB cells. These apparent contradictory
447 findings, suggest that the growth defect and the reduction of TORC1 activity in *FASN*
448 mutants are not due to the addition of cell-autonomous effects but potentially to a
449 systemic regulation, as for instance, Ilp secretion by neurosecretory cells (RULIFSON *et*
450 *al.* 2002). Alternatively, considering that TORC1 directly responds to nutrients (OLDHAM
451 *et al.* 2000), the drop of TORC1 activity may be a consequence of feeding, consistent

with the decrease in food uptake previously reported in *FASN*$^{1-2}$ mutants (GARRIDO *et al.* 2015). Congruently, a study on the transcription factor Mondo, which stimulates glycolysis and FA synthesis in response to dietary sugar (MATTILA *et al.* 2015; RICHARDS *et al.* 2017), suggests the existence of a FASN-dependent control of food intake (SASSU *et al.* 2012). Finally, the drop of TORC1 activity observed in *FASN*$^{1-2}$ mutants may be a consequence of malonyl-CoA accumulation, since mTOR malonylation has been reported to inhibit mTORC1- but not Ilp/mTORC2-dependent activity (BRUNING *et al.* 2018). Whether TOR malonylation and the subsequent decrease in TORC1 activity may also occur in *Drosophila* should be investigated in the future.

Our study reveals that over-activation of mTORC1 and of Ilp signaling, results in a decrease in glycogen stores and in circulating trehalose, suggesting that activation of either signaling branch enhances glucose consumption to sustain cell growth. However, the activation of neither mTORC1 nor Ilp signaling induces an increase in body weight. Ubiquitous activation of TORC1 or Ilp signaling is likely to promote the growth of most cells, but might concurrently perturb endocrine signals dampening overall growth. For instance, previous studies reported that activation of Ilp signaling within the ecdysone-secreting gland, results in a systemic decrease in body growth (CALDWELL *et al.* 2005; COLOMBANI *et al.* 2005; MIRTH 2005). Of note, we observed that larvae fed a 20%-SSD result in pupae with reduced body weight, an effect that is partially suppressed when either TORC1 or Ilp signaling is over-activated. The fact that the overall body weight of these animals is maintained within a range likely compatible with organismal survival contrasts with the observed high rate of lethality. The decrease in glycogen and trehalose suggests that in these animals each cell tends to increase its basal metabolism evoking an egoist behavior that might perturb the equilibrium between cell-autonomous and systemic regulation. Thus, in a stressful situation, as when animals are

fed a 20%-SSD, the need of a tight adjustment to an unbalanced diet might enhance the distortion between cell-autonomous effects and systemic regulation, resulting in animal death.

A plethora of studies in mammalian cells indicate that mTOR activation directs metabolism towards glucose consumption, storage and anabolism (GOTTLOB *et al.* 2001; INOKI *et al.* 2003b; HAHN-WINDGASSEN *et al.* 2005; DUVEL *et al.* 2010; PETERSON *et al.* 2011; HOUDDANE *et al.* 2017; JALDIN-FINCATI *et al.* 2017; WIPPERMAN *et al.* 2019). Our study suggests that in the *Drosophila* larvae, TOR promotes glucose consumption, but an increase in TAG levels is observed only for larvae fed a 20%-SSD when Ilp signaling is ubiquitously over-activated. However, at the cell-autonomous level, we observe that inhibition of glycolysis or FA synthesis restrains neither larval FB cell growth nor overgrowth induced by TORC1 stimulation in these cells. These findings counteract the idea that mTORC1 potentiates a glycolysis/FA synthesis axis (DUVEL *et al.* 2010) to sustain cell growth. To overcome the lack of glycolytic products and of membrane lipids, these cells may benefit of a transfer from neighboring cells and/or might favor alternative metabolic pathways, including glutamine catabolism to feed TCA anaplerosis, which has been shown to be a crucial pathway in mTORC1-stimulated mammalian cells (CHOO *et al.* 2010; CSIBI *et al.* 2013; CSIBI *et al.* 2014). Nonetheless, such compensatory processes do not fully operate to sustain Ilp-dependent overgrowth, potentially because these cells might be more sensitive to homeostasis perturbations or because the modulation of Ilp signaling would be required for these compensatory processes.

As a coordinator of growth and metabolism, mTOR plays a central role in tumor development (DOWLING *et al.* 2010; HARACHI *et al.* 2018; MOSSMANN *et al.* 2018; TIAN *et al.* 2019). PTEN, the tumor suppressor that counteracts PI3K activity downstream of the

Ilp receptor, is deficient in several human cancers (CULLY *et al.* 2006). Mutation of TSC1 or TSC2, which results in mTORC1 hyper-activation, is associated with benign tumors but also with brain, kidney and lung destructive diseases (HENSKE *et al.* 2016). To investigate the role of mTOR regarding tumor development, a recent study reported the generation of liver-specific double knockout mice for TSC1 and PTEN (GURI *et al.* 2017). These mice develop hepatic steatosis that eventually progresses to hepatocellular carcinoma. Both processes are suppressed in mice fed the mTORC1/2 inhibitors INK128, but not the mTORC1 inhibitor rapamycin, supporting an Ilp/mTORC2 specific effect. The combination of inhibitors against mTOR and metabolism is currently under clinical investigation to fight cancers (MOSSMANN *et al.* 2018). Importantly, our study reveals that ubiquitous inhibition of basal metabolism produces dramatic effects during development, while at the cell-autonomous level, it only moderates growth induced by over-activation of Ilp/TORC2 signaling. Therefore, the use of drug therapy to fight cancer must be taken with caution, in particular if organismal development is not complete and most efforts should be made to selectively target sick tissues.

AKNOWLEDGMENTS

We wish to thank D Petit for preparing the fly media, H Stocker for fly stocks, A Teleman for the phospho-S6 antibody, M Gettings for editing the manuscript, and the NIG and VDRC stock centers for RNAi fly strains. We wish to thank the *French government* for fellowship to MD (MENRT 2015-155) and DG (MRT 2011-78), the *Fondation pour la Recherche Médicale* for fellowship to DG (FDT201 4093 0800), the *Fondation ARC* for grant support to JM (projet ARC 1555286) and the *Ligue de Recherche contre le Cancer* for grant support to JM (M27218). The authors declare no competing financial interests.

AUTHOR CONTRIBUTIONS

JM designed the experiments; MD, DG, MP, TR and JM performed the experiments; MD, DG, ALR and JM analyzed the results; and JM wrote the manuscript.

FIGURE LEGENDS

Figure 1: TORC1- and Ilp-dependent growth in FB cells. MARCM clones labeled by GFP (green) in the FB of L3 larvae. Nuclei were labeled with DAPI (silver) and membranes with phalloidin (red). Control (A), *Rheb*$^{+}$ (B), *PTEN*$^{-/-}$ (C) and *PTEN*$^{-/-}$;*Rheb*$^{+}$ (D) clones were generated in a wild type background. *Rheb*$^{+}$ (E), *PTEN*$^{-/-}$ (F), *Tor*^{2L1} (G) *Tor*^{2L1}, *Rheb*$^{+}$ (H) *Tor*^{2L1},*PTEN*$^{-/-}$ (I), *Tor*$^{\Delta P}$ (J), *Tor*$^{\Delta P}$,*Rheb*$^{+}$ (K), *Tor*$^{\Delta P}$,*PTEN*$^{-/-}$ (L) *Tor*^{2L19} (M) *Tor*^{2L19}, *Rheb*$^{+}$ (N) and *Tor*^{2L19},*PTEN*$^{-/-}$ (O), clones were generated in a *Minute* (*M*) background. Scale bars: 50µm.

Figure 2: TORC1 and Ilp signaling activity in FB cells. (**A-J**) MARCM clones labeled by GFP (green) in the FB of L3 larvae. Clones were generated in a wild type (A,E,I,J,K,L) or a *Minute* (B,C,D,F,G,H) background and nuclei were labeled with DAPI (silver). FB tissues with *PTEN*$^{-/-}$ (A), *Tor*^{2L1} (B), *Tor*$^{\Delta P}$ (C), *Tor*^{2L19} (D) and *FASN*$^{1-2}$ (K) clones were stained with a phospho-AKT antibody. FB tissues with control (E), *Tor*^{2L1} (F), *Tor*$^{\Delta P}$ (G), *Tor*^{2L19} (H) *Rheb*$^{+}$ (I), *PTEN*$^{-/-}$ (J) and *FASN*$^{1-2}$ (L) clones were stained with a phospho-S6 antibody. Scale bars: 50µm. (**M**) Percentage of P-S6 positive clones with respect to the total number of MARCM clones for control, *FASN*$^{1-2}$, *PTEN*$^{-/-}$, *Rheb*$^{+}$, *Tor*^{2L1}, *Tor*$^{\Delta P}$ and *Tor*^{2L19} genotypes.

551 **Figure 3: Enhanced TORC1 or Ilp signaling affects larval metabolism.** (**A-B**) Body
552 weight of female (A) and male (B) prepupae formed from larvae fed either a standard
553 (0%) or a 20%-SSD (20%) as from the L2/L3 transition. (**C-F**) Measurement of total
554 protein (C), TAG (D), glycogen (E) and trehalose (F) levels in prepupae fed either a
555 standard or a 20%-SSD. Prepupae used in these measurements were the F1 progeny
556 from *da-gal4*;*UAS-Dcr-2* females mated to either control (Co), *EP(UAS)-Rheb* (*Rheb*$^{++}$)
557 or *UAS-PTEN-RNAi* (*PTEN-Ri*) males.

558

559 **Figure 4: Glycolysis knockdown in whole organisms.** (**A**) Scheme of basal
560 metabolism. Glucose and trehalose enter glycolysis as glucose-6P, whereas fructose
561 follows a distinct pathway to triose-P. Enzymes investigated in the present study are
562 marked in red. (**B**) Phenotype of ubiquitous RNAi knockdown of PFK1, PK, LDH and
563 PDH. Flies were left to lay eggs overnight either at 29°C (column 0h) or at 19°C and
564 transferred to 29°C the day after (column 24h); then development proceeded at 29°C
565 (i.e. the temperature that inactivates Gal80). (**C**) Western-blot analysis of total (top) or
566 phosphorylated (mid) dS6K (left) or Akt (right) proteins; tubulin (bottom) was used as a
567 loading control. Protein extracts were prepared with late L2 larvae either control (Co), or
568 expressing RNAi against the indicated metabolic enzymes. (**D**) Survival at 29°C of male
569 (top) and female (bottom) control flies or flies expressing RNAi against the indicated
570 metabolic enzymes as from adult eclosion.

571

572 **Figure 5: Cell-autonomous requirement of glycolysis for Ilp- but not TORC1-**
573 **dependent overgrowth.** (**A-G**) MARCM clones labeled by GFP (green) in the FB of L3
574 larvae. Nuclei were labeled with DAPI (silver) and membranes with phalloidin (red).
575 Genotypes of MARCM clones are: *PFK1-RNAi* (A), *PK-RNAi* (B), *LDH-RNAi* (C), *PDH-*

RNAi (D), *Rheb*$^{+}$,*PFK1-RNAi* (E), *Rheb*$^{+}$,*PK-RNAi* (F), *Rheb*$^{+}$,*LDH-RNAi* (G), *Rheb*$^{+}$,*PDH-RNAi* (H), *PTEN*$^{-/-}$;*PFK1-RNAi* (I), *PTEN*$^{-/-}$;*PK-RNAi* (J), *PTEN*$^{-/-}$;*PDH-RNAi* (K) and *PTEN*$^{-/-}$;*PDH-RNAi* (L). Scale bars: 50µm. (**M**) Relative size of clonal cells corresponding to the clones shown in A-L, and in Figure 1A for control (Co).

Figure 6: *FASN*$^{1-2}$ mutation affects developmental growth and TORC1 signaling. (**A**) Developmental duration from egg laying to metamorphosis onset of *w*^{1118} control (Co) and *FASN*$^{1-2}$ (FASN) larvae fed either a beySD (0%) or a 10% sucrose-supplemented-beySD as from the L2/L3 transition (10%); n: total number of larvae collected for each condition. Each condition and genotype significantly differ from each other, either by final frequency or dynamic of pupariation (Table S6). (**B**) Prepupal weight of females (left) and males (right) as listed in 6A; the numbers of weighted prepupae are indicated above each sample. (**C**) Western-blot analysis of (from top to bottom) total dS6K, phosphorylated dS6K, total Akt, phosphorylated Akt and total tubulin as a loading control. Protein extracts were prepared from feeding L3 larvae prior to the wandering stage as listed in 6A. For each condition, at least 30 larvae were used to prepare protein extracts.

Figure 7: Cell-autonomous requirement of FASN activity for Ilp- but not TORC1-dependent overgrowth. (**A-L**) MARCM clones labeled by GFP (green) in the FB of L3 larvae fed either a standard (A-C, G-I) or a 20%-SSD (D-F, J-L). Nuclei were labeled with DAPI (silver) and membranes with phalloidin (red). Genotypes of MARCM clones are: *Rheb*$^{+}$ (A,D), *PTEN*$^{-/-}$ (B,E) *PTEN*$^{-/-}$,*Rheb*$^{+}$ (C,F), *FASN*$^{1-2}$;*Rheb*$^{+}$ (G,J) *FASN*$^{1-2}$,*PTEN*$^{-/-}$ (H,K) and the *FASN*$^{1-2}$,*PTEN*$^{-/-}$;*Rheb*$^{+}$ (I,L). Scale bars: 50µm. (**M**) Relative

size of clonal cells corresponding to the clones shown in A-L and in Figure S5A-D for *FASN*$^{1-2}$ and *PTEN-RNAi* clones and in Figure 1A for control (Co).

LITERATURE CITED

Antikainen, H., M. Driscoll, G. Haspel and R. Dobrowolski, 2017 TOR-mediated regulation of metabolism in aging. Aging Cell 16**:** 1219-1233.

Bohni, R., J. Riesgo-Escovar, S. Oldham, W. Brogiolo, H. Stocker *et al.*, 1999 Autonomous control of cell and organ size by CHICO, a Drosophila homolog of vertebrate IRS1-4. Cell 97**:** 865-875.

Britton, J. S., W. K. Lockwood, L. Li, S. M. Cohen and B. A. Edgar, 2002 Drosophila's insulin/PI3-kinase pathway coordinates cellular metabolism with nutritional conditions. Dev Cell 2**:** 239-249.

Bruning, U., F. Morales-Rodriguez, J. Kalucka, J. Goveia, F. Taverna *et al.*, 2018 Impairment of Angiogenesis by Fatty Acid Synthase Inhibition Involves mTOR Malonylation. Cell Metab 28**:** 866-880 e815.

Caldwell, P. E., M. Walkiewicz and M. Stern, 2005 Ras activity in the Drosophila prothoracic gland regulates body size and developmental rate via ecdysone release. Curr Biol 15**:** 1785-1795.

Caron, A., D. Richard and M. Laplante, 2015 The Roles of mTOR Complexes in Lipid Metabolism. Annu Rev Nutr 35**:** 321-348.

Choo, A. Y., S. G. Kim, M. G. Vander Heiden, S. J. Mahoney, H. Vu *et al.*, 2010 Glucose addiction of TSC null cells is caused by failed mTORC1-dependent balancing of metabolic demand with supply. Mol Cell 38**:** 487-499.

623 Chung, H., D. W. Loehlin, H. D. Dufour, K. Vaccarro, J. G. Millar *et al.*, 2014 A single
624 gene affects both ecological divergence and mate choice in Drosophila. Science
625 343**:** 1148-1151.

626 Colombani, J., L. Bianchini, S. Layalle, E. Pondeville, C. Dauphin-Villemant *et al.*, 2005
627 Antagonistic actions of ecdysone and insulins determine final size in Drosophila.
628 Science 310**:** 667-670.

629 Csibi, A., S. M. Fendt, C. Li, G. Poulogiannis, A. Y. Choo *et al.*, 2013 The mTORC1
630 pathway stimulates glutamine metabolism and cell proliferation by repressing
631 SIRT4. Cell 153**:** 840-854.

632 Csibi, A., G. Lee, S. O. Yoon, H. Tong, D. Ilter *et al.*, 2014 The mTORC1/S6K1 pathway
633 regulates glutamine metabolism through the eIF4B-dependent control of c-Myc
634 translation. Curr Biol 24**:** 2274-2280.

635 Cully, M., H. You, A. J. Levine and T. W. Mak, 2006 Beyond PTEN mutations: the PI3K
636 pathway as an integrator of multiple inputs during tumorigenesis. Nat Rev Cancer
637 6**:** 184-192.

638 Dibble, C. C., W. Elis, S. Menon, W. Qin, J. Klekota *et al.*, 2012 TBC1D7 is a third
639 subunit of the TSC1-TSC2 complex upstream of mTORC1. Mol Cell 47**:** 535-546.

640 Dibble, C. C., and B. D. Manning, 2013 Signal integration by mTORC1 coordinates
641 nutrient input with biosynthetic output. Nat Cell Biol 15**:** 555-564.

642 Dietzl, G., D. Chen, F. Schnorrer, K. C. Su, Y. Barinova *et al.*, 2007 A genome-wide
643 transgenic RNAi library for conditional gene inactivation in Drosophila. Nature
644 448**:** 151-156.

645 Dong, J., and D. Pan, 2004 Tsc2 is not a critical target of Akt during normal Drosophila
646 development. Genes Dev 18**:** 2479-2484.

Dowling, R. J., I. Topisirovic, B. D. Fonseca and N. Sonenberg, 2010 Dissecting the role of mTOR: lessons from mTOR inhibitors. Biochim Biophys Acta 1804**:** 433-439.

Duvel, K., J. L. Yecies, S. Menon, P. Raman, A. I. Lipovsky *et al.*, 2010 Activation of a metabolic gene regulatory network downstream of mTOR complex 1. Mol Cell 39**:** 171-183.

Edgar, B. A., and T. L. Orr-Weaver, 2001 Endoreplication cell cycles: more for less. Cell 105**:** 297-306.

Engelman, J. A., J. Luo and L. C. Cantley, 2006 The evolution of phosphatidylinositol 3-kinases as regulators of growth and metabolism. Nat Rev Genet 7**:** 606-619.

Garami, A., F. J. Zwartkruis, T. Nobukuni, M. Joaquin, M. Roccio *et al.*, 2003 Insulin activation of Rheb, a mediator of mTOR/S6K/4E-BP signaling, is inhibited by TSC1 and 2. Mol Cell 11**:** 1457-1466.

Garrido, D., T. Rubin, M. Poidevin, B. Maroni, A. Le Rouzic *et al.*, 2015 Fatty Acid Synthase Cooperates with Glyoxalase 1 to Protect against Sugar Toxicity. PLoS Genet 11**:** e1004995.

Goberdhan, D. C., M. H. Ogmundsdottir, S. Kazi, B. Reynolds, S. M. Visvalingam *et al.*, 2009 Amino acid sensing and mTOR regulation: inside or out? Biochem Soc Trans 37**:** 248-252.

Gottlob, K., N. Majewski, S. Kennedy, E. Kandel, R. B. Robey *et al.*, 2001 Inhibition of early apoptotic events by Akt/PKB is dependent on the first committed step of glycolysis and mitochondrial hexokinase. Genes Dev 15**:** 1406-1418.

Groenewoud, M. J., and F. J. Zwartkruis, 2013 Rheb and mammalian target of rapamycin in mitochondrial homoeostasis. Open Biol 3**:** 130185.

Guri, Y., M. Colombi, E. Dazert, S. K. Hindupur, J. Roszik *et al.*, 2017 mTORC2 Promotes Tumorigenesis via Lipid Synthesis. Cancer Cell 32**:** 807-823 e812.

Haeusler, R. A., T. E. McGraw and D. Accili, 2018 Biochemical and cellular properties of insulin receptor signalling. Nat Rev Mol Cell Biol 19**:** 31-44.

Hagiwara, A., M. Cornu, N. Cybulski, P. Polak, C. Betz *et al.*, 2012 Hepatic mTORC2 activates glycolysis and lipogenesis through Akt, glucokinase, and SREBP1c. Cell Metab 15**:** 725-738.

Hahn-Windgassen, A., V. Nogueira, C. C. Chen, J. E. Skeen, N. Sonenberg *et al.*, 2005 Akt activates the mammalian target of rapamycin by regulating cellular ATP level and AMPK activity. J Biol Chem 280**:** 32081-32089.

Harachi, M., K. Masui, Y. Okamura, R. Tsukui, P. S. Mischel *et al.*, 2018 mTOR Complexes as a Nutrient Sensor for Driving Cancer Progression. Int J Mol Sci 19.

Hay, N., and N. Sonenberg, 2004 Upstream and downstream of mTOR. Genes Dev 18**:** 1926-1945.

Henske, E. P., S. Jozwiak, J. C. Kingswood, J. R. Sampson and E. A. Thiele, 2016 Tuberous sclerosis complex. Nat Rev Dis Primers 2**:** 16035.

Hietakangas, V., and S. M. Cohen, 2007 Re-evaluating AKT regulation: role of TOR complex 2 in tissue growth. Genes Dev 21**:** 632-637.

Houddane, A., L. Bultot, L. Novellasdemunt, M. Johanns, M. A. Gueuning *et al.*, 2017 Role of Akt/PKB and PFKFB isoenzymes in the control of glycolysis, cell proliferation and protein synthesis in mitogen-stimulated thymocytes. Cell Signal 34**:** 23-37.

693 Howell, J. J., S. J. Ricoult, I. Ben-Sahra and B. D. Manning, 2013 A growing role for
694 mTOR in promoting anabolic metabolism. Biochem Soc Trans 41**:** 906-912.

695 Inoki, K., Y. Li, T. Xu and K. L. Guan, 2003a Rheb GTPase is a direct target of TSC2
696 GAP activity and regulates mTOR signaling. Genes Dev 17**:** 1829-1834.

697 Inoki, K., T. Zhu and K. L. Guan, 2003b TSC2 mediates cellular energy response to
698 control cell growth and survival. Cell 115**:** 577-590.

699 Jaldin-Fincati, J. R., M. Pavarotti, S. Frendo-Cumbo, P. J. Bilan and A. Klip, 2017
700 Update on GLUT4 Vesicle Traffic: A Cornerstone of Insulin Action. Trends
701 Endocrinol Metab 28**:** 597-611.

702 Kim, D. H., D. D. Sarbassov, S. M. Ali, J. E. King, R. R. Latek *et al.*, 2002 mTOR
703 interacts with raptor to form a nutrient-sensitive complex that signals to the cell
704 growth machinery. Cell 110**:** 163-175.

705 Lamming, D. W., and D. M. Sabatini, 2013 A Central role for mTOR in lipid
706 homeostasis. Cell Metab 18**:** 465-469.

707 Laplante, M., and D. M. Sabatini, 2012 mTOR signaling in growth control and disease.
708 Cell 149**:** 274-293.

709 Lee, T., and L. Luo, 2001 Mosaic analysis with a repressible cell marker (MARCM) for
710 Drosophila neural development. Trends Neurosci 24**:** 251-254.

711 Lehmann, M., 2018 Endocrine and physiological regulation of neutral fat storage in
712 Drosophila. Mol Cell Endocrinol 461**:** 165-177.

713 Lien, E. C., C. C. Dibble and A. Toker, 2017 PI3K signaling in cancer: beyond AKT. Curr
714 Opin Cell Biol 45**:** 62-71.

715 Ma, X. M., and J. Blenis, 2009 Molecular mechanisms of mTOR-mediated translational
716 control. Nat Rev Mol Cell Biol 10**:** 307-318.

717 Magnuson, B., B. Ekim and D. C. Fingar, 2012 Regulation and function of ribosomal
718 protein S6 kinase (S6K) within mTOR signalling networks. Biochem J 441**:** 1-21.

719 Majewski, N., V. Nogueira, P. Bhaskar, P. E. Coy, J. E. Skeen *et al.*, 2004 Hexokinase-
720 mitochondria interaction mediated by Akt is required to inhibit apoptosis in the
721 presence or absence of Bax and Bak. Mol Cell 16**:** 819-830.

722 Mattila, J., E. Havula, E. Suominen, M. Teesalu, I. Surakka *et al.*, 2015 Mondo-Mlx
723 Mediates Organismal Sugar Sensing through the Gli-Similar Transcription Factor
724 Sugarbabe. Cell Rep 13**:** 350-364.

725 McManus, E. J., K. Sakamoto, L. J. Armit, L. Ronaldson, N. Shpiro *et al.*, 2005 Role that
726 phosphorylation of GSK3 plays in insulin and Wnt signalling defined by knockin
727 analysis. EMBO J 24**:** 1571-1583.

728 Mirth, C., 2005 Ecdysteroid control of metamorphosis in the differentiating adult leg
729 structures of Drosophila melanogaster. Dev Biol 278**:** 163-174.

730 Montagne, J., 2016 A Wacky Bridge to mTORC1 Dimerization. Dev Cell 36**:** 129-130.

731 Montagne, J., C. Lecerf, J. P. Parvy, J. M. Bennion, T. Radimerski *et al.*, 2010 The
732 nuclear receptor DHR3 modulates dS6 kinase-dependent growth in Drosophila.
733 PLoS Genet 6**:** e1000937.

734 Montagne, J., T. Radimerski and G. Thomas, 2001 Insulin signaling: lessons from the
735 Drosophila tuberous sclerosis complex, a tumor suppressor. Sci STKE 2001**:**
736 PE36.

737 Montagne, J., M. J. Stewart, H. Stocker, E. Hafen, S. C. Kozma *et al.*, 1999 Drosophila
738 S6 kinase: a regulator of cell size. Science 285**:** 2126-2129.

739 Montagne, J., and G. Thomas, 2004 S6K integrates nutrient and mitogen signals to
740 control cell growth. , pp. 265-298 in *Cell growth: control of cell size.*, edited by M.
741 Hall, Raff, M., Thomas, G. Cold Spring Harbor Press.

742 Mossmann, D., S. Park and M. N. Hall, 2018 mTOR signalling and cellular metabolism
743 are mutual determinants in cancer. Nat Rev Cancer 18**:** 744-757.

744 Nakae, J., T. Kitamura, D. L. Silver and D. Accili, 2001 The forkhead transcription factor
745 Foxo1 (Fkhr) confers insulin sensitivity onto glucose-6-phosphatase expression.
746 J Clin Invest 108**:** 1359-1367.

747 Oldham, S., J. Montagne, T. Radimerski, G. Thomas and E. Hafen, 2000 Genetic and
748 biochemical characterization of dTOR, the Drosophila homolog of the target of
749 rapamycin. Genes Dev 14**:** 2689-2694.

750 Padmanabha, D., and K. D. Baker, 2014 Drosophila gains traction as a repurposed tool
751 to investigate metabolism. Trends Endocrinol Metab 25**:** 518-527.

752 Pallares-Cartes, C., G. Cakan-Akdogan and A. A. Teleman, 2012 Tissue-specific
753 coupling between insulin/IGF and TORC1 signaling via PRAS40 in Drosophila.
754 Dev Cell 22**:** 172-182.

755 Parvy, J. P., L. Napal, T. Rubin, M. Poidevin, L. Perrin *et al.*, 2012 Drosophila
756 melanogaster Acetyl-CoA-carboxylase sustains a fatty acid-dependent remote
757 signal to waterproof the respiratory system. PLoS Genet 8**:** e1002925.

758 Parvy, J. P., P. Wang, D. Garrido, A. Maria, C. Blais *et al.*, 2014 Forward and feedback
759 regulation of cyclic steroid production in Drosophila melanogaster. Development
760 141**:** 3955-3965.

761 Peterson, T. R., S. S. Sengupta, T. E. Harris, A. E. Carmack, S. A. Kang *et al.*, 2011
762 mTOR complex 1 regulates lipin 1 localization to control the SREBP pathway.
763 Cell 146**:** 408-420.

764 Polak, P., N. Cybulski, J. N. Feige, J. Auwerx, M. A. Ruegg *et al.*, 2008 Adipose-specific
765 knockout of raptor results in lean mice with enhanced mitochondrial respiration.
766 Cell Metab 8**:** 399-410.

767 Radimerski, T., J. Montagne, M. Hemmings-Mieszczak and G. Thomas, 2002a Lethality
768 of Drosophila lacking TSC tumor suppressor function rescued by reducing dS6K
769 signaling. Genes Dev 16**:** 2627-2632.

770 Radimerski, T., J. Montagne, F. Rintelen, H. Stocker, J. van der Kaay *et al.*, 2002b
771 dS6K-regulated cell growth is dPKB/dPI(3)K-independent, but requires dPDK1.
772 Nat Cell Biol 4**:** 251-255.

773 Richards, P., S. Ourabah, J. Montagne, A. F. Burnol, C. Postic *et al.*, 2017
774 MondoA/ChREBP: The usual suspects of transcriptional glucose sensing;
775 Implication in pathophysiology. Metabolism 70**:** 133-151.

776 Robey, R. B., and N. Hay, 2009 Is Akt the "Warburg kinase"?-Akt-energy metabolism
777 interactions and oncogenesis. Semin Cancer Biol 19**:** 25-31.

778 Romero-Pozuelo, J., C. Demetriades, P. Schroeder and A. A. Teleman, 2017
779 CycD/Cdk4 and Discontinuities in Dpp Signaling Activate TORC1 in the
780 Drosophila Wing Disc. Dev Cell 42**:** 376-387 e375.

781 Rulifson, E. J., S. K. Kim and R. Nusse, 2002 Ablation of insulin-producing neurons in
782 flies: growth and diabetic phenotypes. Science 296**:** 1118-1120.

783 Sarbassov, D. D., D. A. Guertin, S. M. Ali and D. M. Sabatini, 2005 Phosphorylation and
784 regulation of Akt/PKB by the rictor-mTOR complex. Science 307**:** 1098-1101.

Sassu, E. D., J. E. McDermott, B. J. Keys, M. Esmaeili, A. C. Keene *et al.*, 2012 Mio/dChREBP coordinately increases fat mass by regulating lipid synthesis and feeding behavior in Drosophila. Biochem Biophys Res Commun 426**:** 43-48.

Saxton, R. A., and D. M. Sabatini, 2017 mTOR Signaling in Growth, Metabolism, and Disease. Cell 168**:** 960-976.

Scott, R. C., O. Schuldiner and T. P. Neufeld, 2004 Role and regulation of starvation-induced autophagy in the Drosophila fat body. Dev Cell 7**:** 167-178.

Shimobayashi, M., and M. N. Hall, 2014 Making new contacts: the mTOR network in metabolism and signalling crosstalk. Nat Rev Mol Cell Biol 15**:** 155-162.

Stocker, H., T. Radimerski, B. Schindelholz, F. Wittwer, P. Belawat *et al.*, 2003 Rheb is an essential regulator of S6K in controlling cell growth in Drosophila. Nat Cell Biol 5**:** 559-565.

Tian, T., X. Li and J. Zhang, 2019 mTOR Signaling in Cancer and mTOR Inhibitors in Solid Tumor Targeting Therapy. Int J Mol Sci 20.

Ugur, B., K. Chen and H. J. Bellen, 2016 Drosophila tools and assays for the study of human diseases. Dis Model Mech 9**:** 235-244.

Wangler, M. F., Y. Hu and J. M. Shulman, 2017 Drosophila and genome-wide association studies: a review and resource for the functional dissection of human complex traits. Dis Model Mech 10**:** 77-88.

Wicker-Thomas, C., D. Garrido, G. Bontonou, L. Napal, N. Mazuras *et al.*, 2015 Flexible origin of hydrocarbon/pheromone precursors in Drosophila melanogaster. J Lipid Res 56**:** 2094-2101.

Wipperman, M. F., D. C. Montrose, A. M. Gotto, Jr. and D. P. Hajjar, 2019 Mammalian Target of Rapamycin: A Metabolic Rheostat for Regulating Adipose Tissue Function and Cardiovascular Health. Am J Pathol 189**:** 492-501.

Yang, H., X. Jiang, B. Li, H. J. Yang, M. Miller *et al.*, 2017 Mechanisms of mTORC1 activation by RHEB and inhibition by PRAS40. Nature 552**:** 368-373.

Yuan, M., E. Pino, L. Wu, M. Kacergis and A. A. Soukas, 2012 Identification of Akt-independent regulation of hepatic lipogenesis by mammalian target of rapamycin (mTOR) complex 2. J Biol Chem 287**:** 29579-29588.

Zhang, H., J. P. Stallock, J. C. Ng, C. Reinhard and T. P. Neufeld, 2000 Regulation of cellular growth by the Drosophila target of rapamycin dTOR. Genes Dev 14**:** 2712-2724.

Zhang, Y., C. J. Billington, Jr., D. Pan and T. P. Neufeld, 2006 Drosophila target of rapamycin kinase functions as a multimer. Genetics 172**:** 355-362.

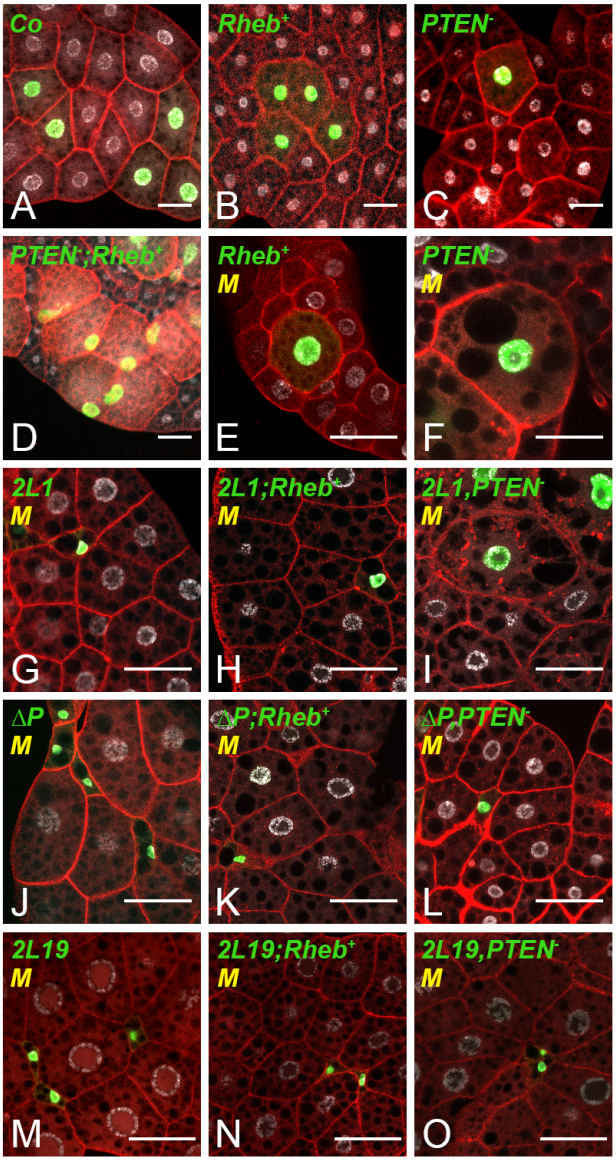
Co
A
Rheb+
B
PTEN-
C
PTEN-;Rheb+
D
Rheb+
M
E
PTEN-
M
F
2L1
M
G
2L1;Rheb
M
H
2L1,PTEN-
M
I
ΔP
M
J
ΔP;Rheb+
M
K
ΔP,PTEN-
M
L
2L19
M
M
2L19;Rheb+
M
N
2L19,PTEN-
M
O

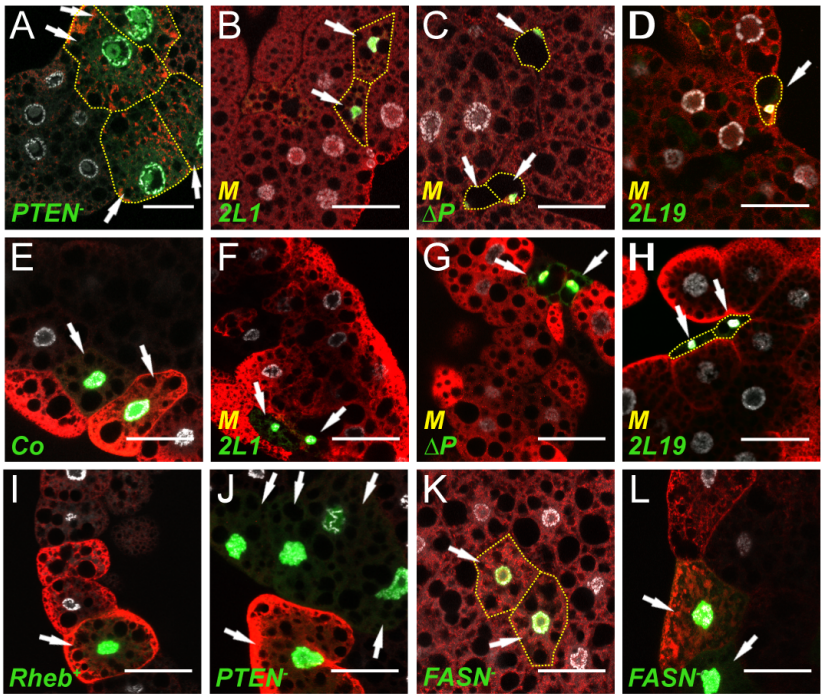
A
PTEN-
B
M
2L1
C
M
ΔP
D
M
2L19
E
Co
F
M
2L1
G
M
ΔP
H
M
2L19
I
Rheb-
J
PTEN-
K
FASN-
L
FASN-

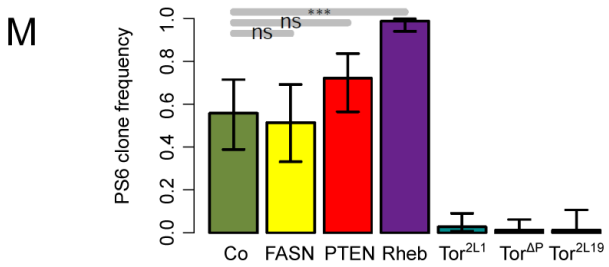
M
PS6 clone frequency
0.0
0.2
0.4
0.6
0.8
1.0
ns
ns
***
Co
FASN
PTEN
Rheb
Tor2L1
TorΔP
Tor2L19

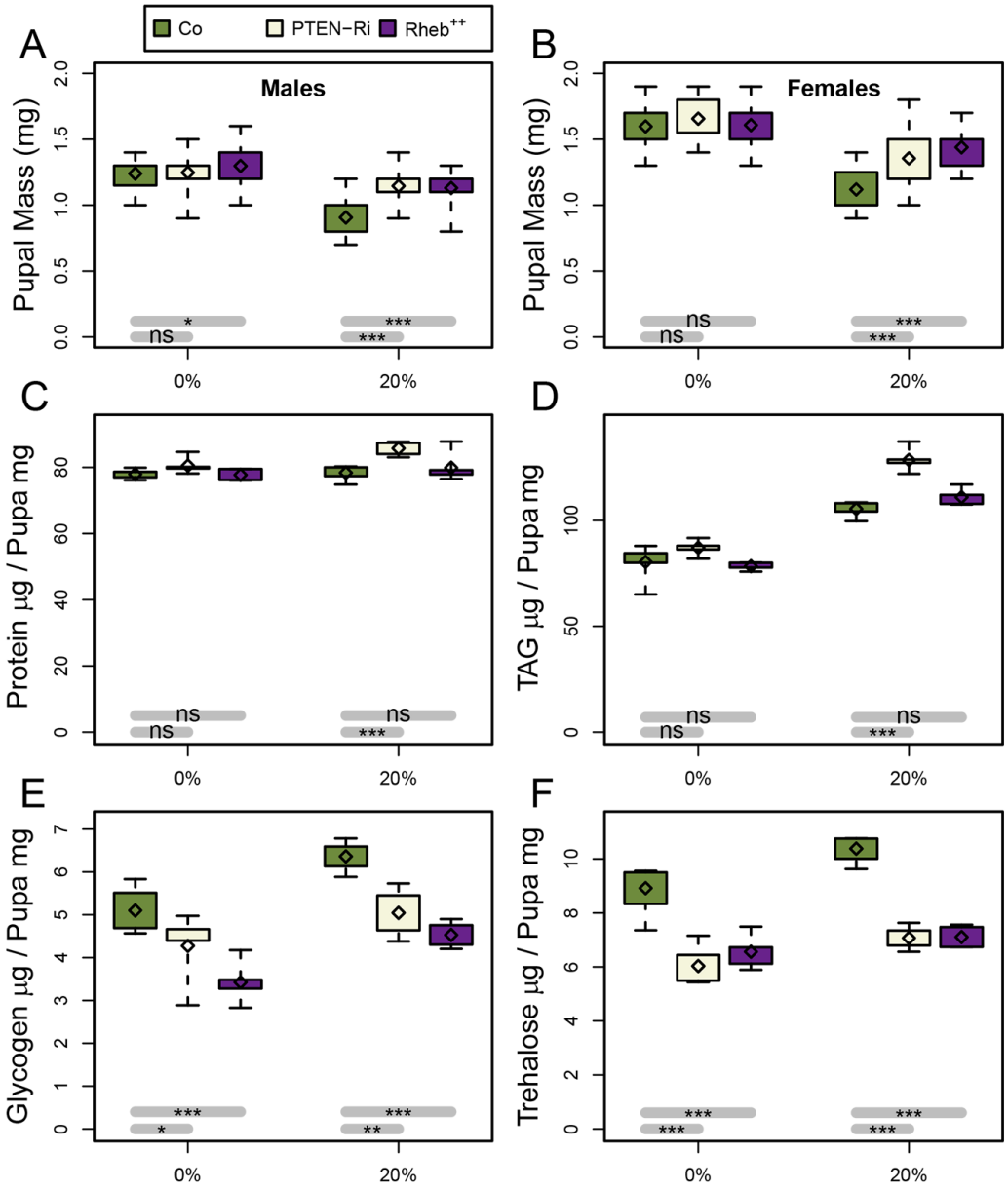
Co
PTEN−Ri
Rheb++
A
Males
Pupal Mass (mg)
0.0
0.5
1.0
1.5
2.0
ns
*
ns
***
***
0%
20%
B
Females
Pupal Mass (mg)
ns
ns
***
***
C
Protein µg / Pupa mg
0
20
40
60
80
ns
ns
ns
***
D
TAG µg / Pupa mg
0
50
100
ns
ns
ns
***
E
Glycogen µg / Pupa mg
0
1
2
3
4
5
6
7
***
*
***
**
F
Trehalose µg / Pupa mg
0
2
4
6
8
10
***
***
***
***

A

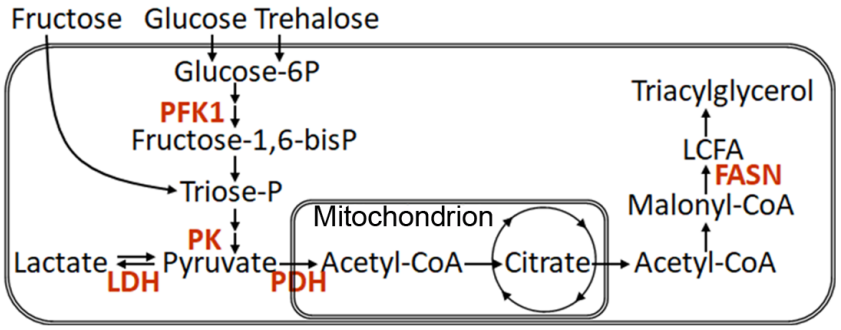

B

19°C>>29°C	0h	24h
PFK1-Ri	† L2/L3	† L3/pp
PK-Ri	† L1/L2	† Late L2
LDH-Ri	† L2/L3	† L3/pp
PDH-Ri	½† L3/pp	½† L3/pp

C

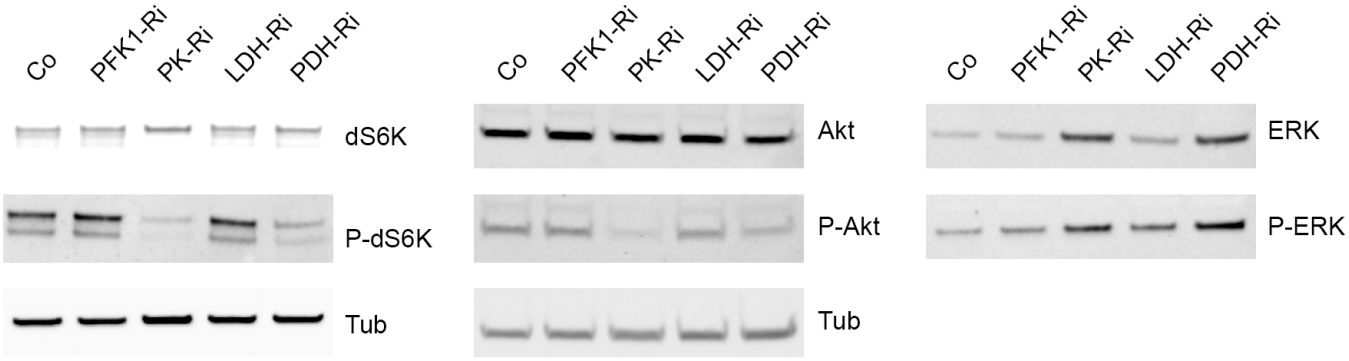

D

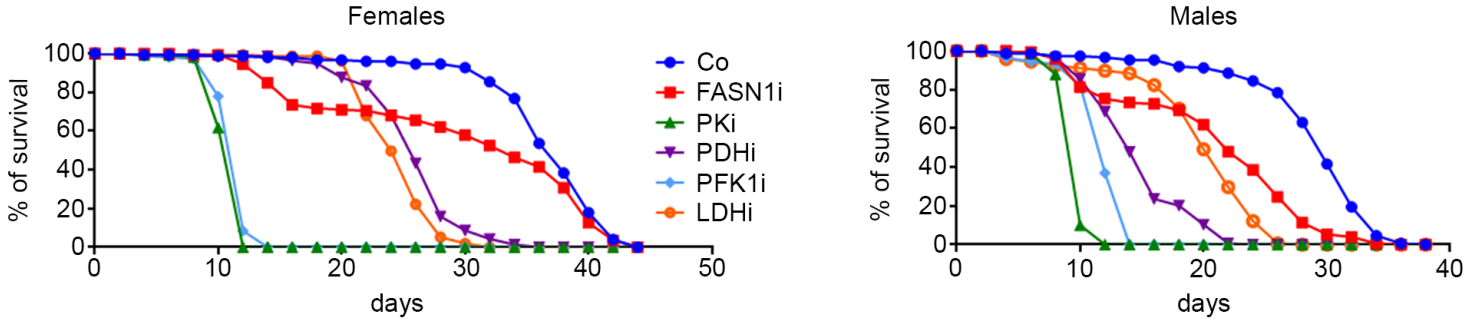

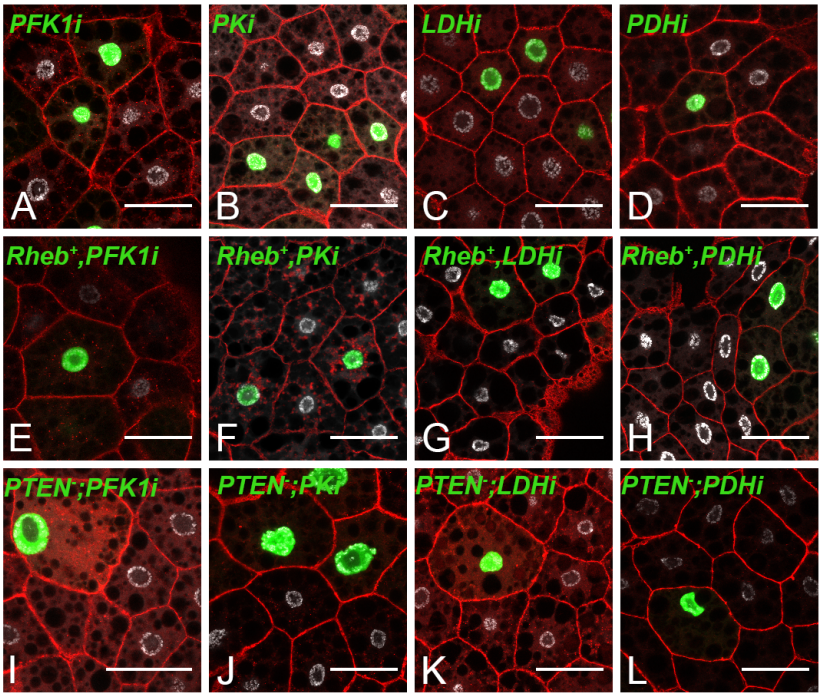
PFK1i
PKi
LDHi
PDHi
A
B
C
D
Rheb+,PFK1i
Rheb+,PKi
Rheb+,LDHi
Rheb+,PDHi
E
F
G
H
PTEN-;PFK1i
PTEN-;PKi
PTEN-;LDHi
PTEN-;PDHi
I
J
K
L

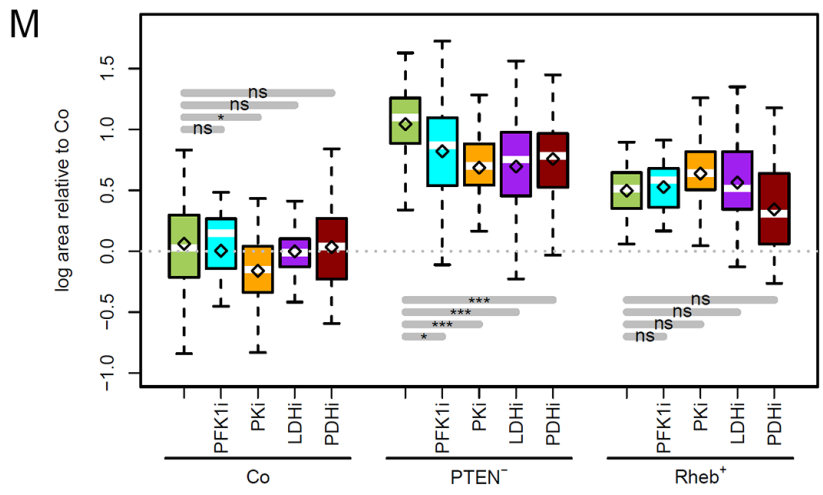
M
log area relative to Co
1.5
1.0
0.5
0.0
−0.5
−1.0
ns
ns
*
ns
***
***
***
*
ns
ns
ns
ns
PFK1i
PKi
LDHi
PDHi
Co
PTEN−
Rheb+

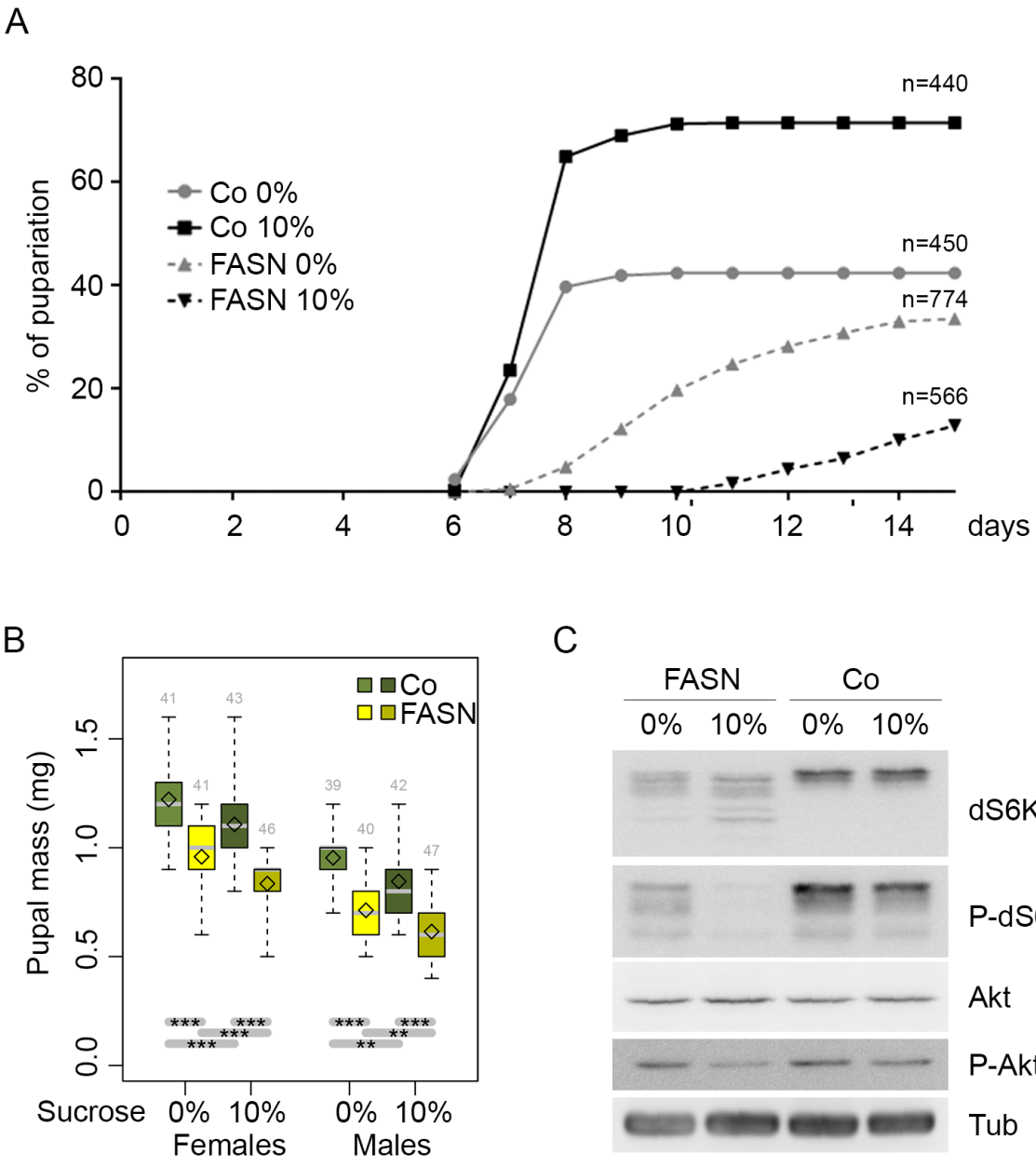
A
80
60
40
20
0
% of pupariation
Co 0%
Co 10%
FASN 0%
FASN 10%
n=440
n=450
n=774
n=566
0
2
4
6
8
10
12
14
days
B
Co
FASN
Pupal mass (mg)
0.0
0.5
1.0
1.5
41
43
41
46
39
40
42
47
***
***
***
***
***
**
Sucrose
0%
10%
0%
10%
Females
Males
C
FASN
Co
0%
10%
0%
10%
dS6K
P-dS6K
Akt
P-Akt
Tub

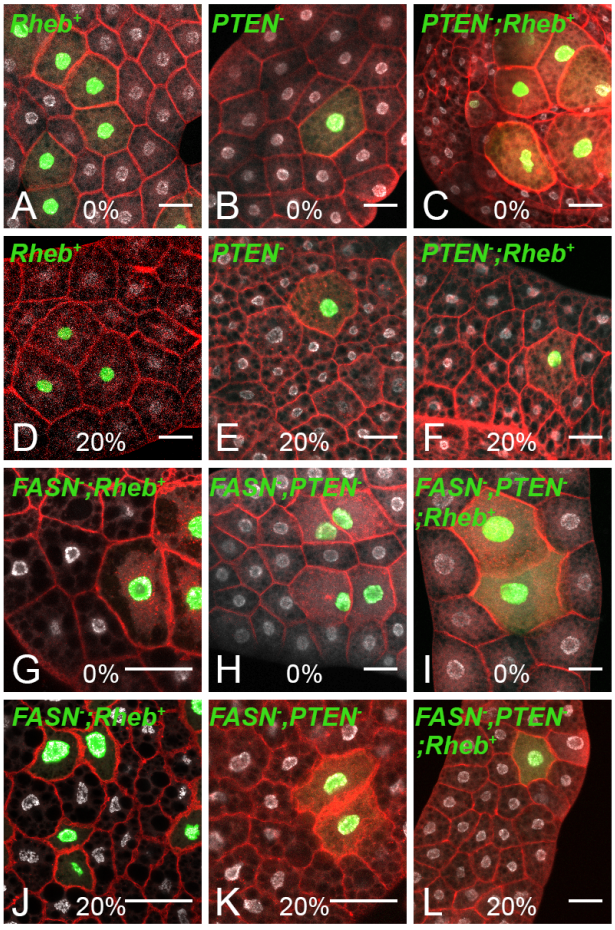
Rheb+
PTEN-
PTEN-;Rheb+
A 0%
B 0%
C 0%
Rheb+
PTEN-
PTEN-;Rheb+
D 20%
E 20%
F 20%
FASN-;Rheb+
FASN-,PTEN-
FASN-,PTEN-
;Rheb+
G 0%
H 0%
I 0%
FASN-;Rheb+
FASN-,PTEN-
FASN-,PTEN+
;Rheb+
J 20%
K 20%
L 20%

M

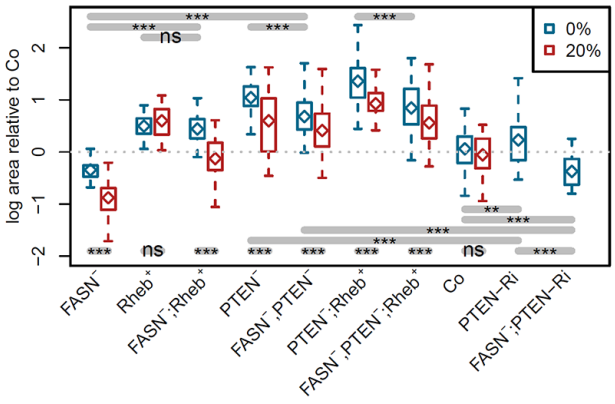
log area relative to Co
0%
20%
ns
FASN-
Rheb+
FASN-;Rheb+
PTEN-
FASN-,PTEN-
PTEN-;Rheb+
FASN-,PTEN-;Rheb+
Co
PTEN-Ri
FASN-;PTEN-Ri